Volume 15
Number 36
28 September 2023
Pages 14685-15062

Nanoscale

rsc.li/nanoscale

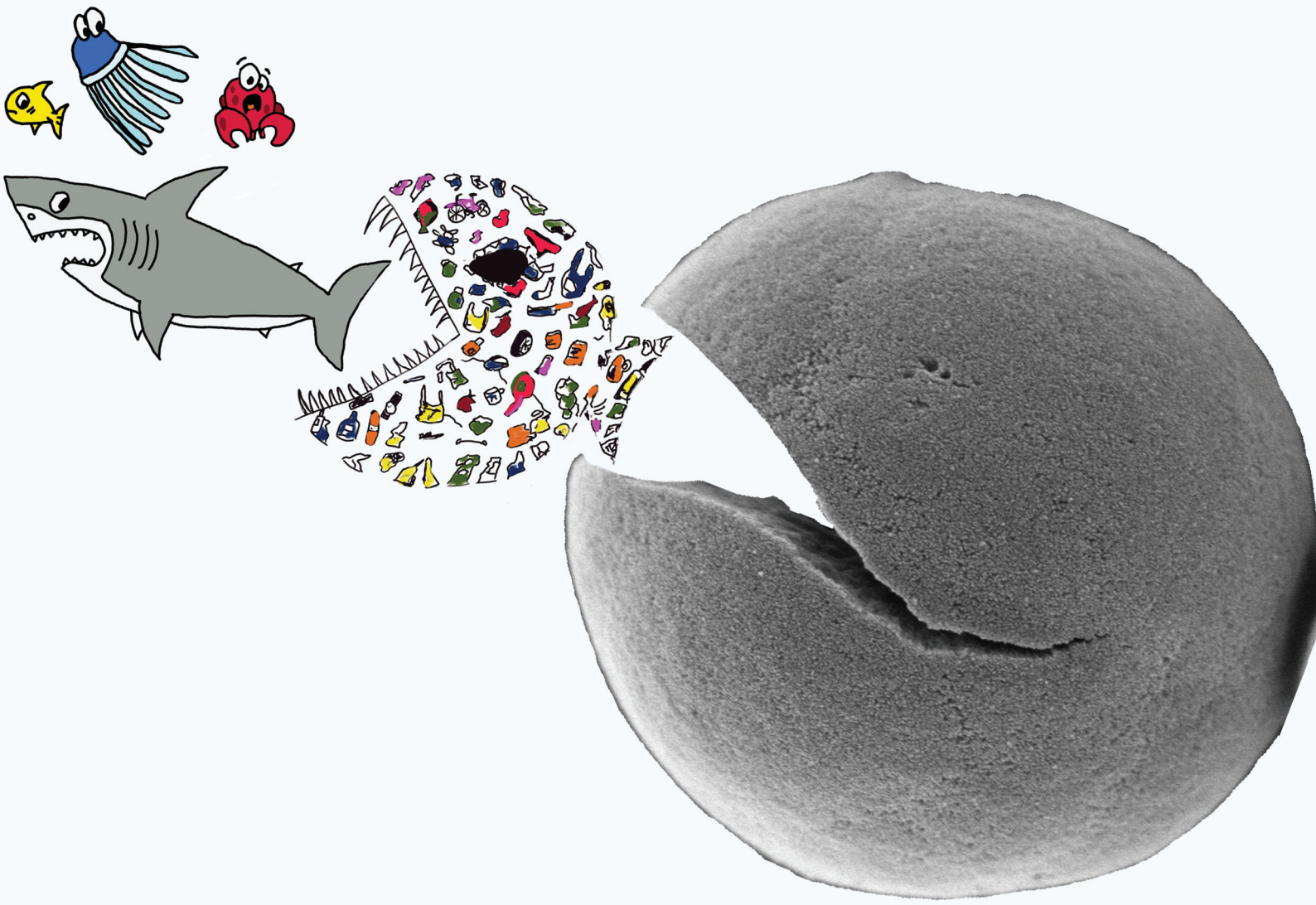

ISSN 2040-3372

ROYAL SOCIETY OF CHEMISTRY

PAPER
Juliane Simmchen *et al.*
Combining photocatalytic collection and degradation of microplastics using self-asymmetric Pac-Man TiO_2

NCNST

Nanoscale

PAPER

View Article Online
View Journal | View Issue

Cite this: *Nanoscale*, 2023, **15**, 14774

Combining photocatalytic collection and degradation of microplastics using self-asymmetric Pac-Man TiO_2†

Purnesh Chattopadhyay, [a] Maria Camila Ariza-Tarazona, [b] Erika Iveth Cedillo-González, [b] Cristina Siligardi[b] and Juliane Simmchen *[a,c]

Received 31st March 2023,
Accepted 5th July 2023

DOI: 10.1039/d3nr01512b

rsc.li/nanoscale

Microplastics are a significant environmental threat and the lack of efficient removal techniques further amplifies this crisis. Photocatalytic semiconducting nanoparticles have the potential to degrade micropollutants, among them microplastics. The hydrodynamic effects leading to the propulsion of micromotors can lead to the accumulation of microplastics in close vicinity of the micromotor. Incorporating these different properties into a single photocatalytic micromotor (self-propulsion, phoretic assembly of passive colloids and photocatalytic oxidation of contaminants), we achieve a highly scalable, inherently-asymmetric Pac-Man TiO_2 micromotor with the ability to actively collect and degrade microplastics. The target microplastics are homogeneous polystyrene microspheres (PS) to facilitate the optical degradation measurements. We cross-correlate the degradation with catalytic activity studies and critically evaluate the timescales required for all involved processes.

1 Introduction

The plastic industry has shown pronounced growth in the last decades. In fact, world plastic production increased from 1.5 to 390.7 million tons from 1950 to 2021.[1,2] The advantages of this material class, such as its low density, durability, excellent barrier properties and relatively low cost, boosted the expansion of this industry. Nowadays, polymer material dominate many fields, including commercial packaging, industrial and construction materials, medicinal uses and municipal applications.[3,4] Even though their robustness was initially celebrated, their long lifetimes make them persistent and difficult to degrade.[5] Due to increased convenience and single-use-habits in large parts of the world, most plastics products have a short useful life and get discarded quickly.[6] Therefore, they enter the environment at high rates that are not matched neither by the rates of natural removal processes nor cleanup actions, leading to accumulation in the environment. Plastic pollution can be reversible when physically removed, but it can become poorly reversible when weathering processes induce the fragmentation of plastic items into micro- and nano-plastic particles.[7] Even though the definition of micro- and nano-plastics has been a subject of debate, plastic fragments with a size ranging from 1 μm to 5 mm are generally defined as microplastics, while those with smaller sizes than 1 μm are listed as nanoplastics.[8]

Micro- and nano-plastics' small size and low weight promotes their transportation and settlement in different environments. As of today, they have been found in marine,[9] and terrestrial systems,[10] as well as in the atmosphere.[11] The concept of a 'microplastic cycle' was introduced to understand better plastic pollution and the fluxes that connect the transport and transformation of microplastic across different compartments of the ecosystem with drastic consequences for many species.[12,13] In this regard, reducing the introduction of microplastics into the marine environment will limit their transport into other ecosystems, which will require governmental and societal changes, connected with increased awareness.

In the mean time, attention to recycling, clean up and the removal of smaller debris *via* wastewater treatment plants (WWTPs) are a critical point source for microplastics in marine ecosystems.[14] As for different emergent pollutants, WWTPs are not yet set up to remove them effectively.[15] For microplastics, this is primarily due to a lack of viability of filtering devices.[16] Furthermore, studies suggest that WWTPs can act as a formation source of micro- and nano-plastics across the different treatment stages. Microplastics undergo

[a]*Chair of Physical Chemistry, TU Dresden, Zellescher Weg 19, Dresden, Germany. E-mail: juliane.simmchen@tu-dresden.de; Fax: +49 351 463-37164; Tel: +49 351 463-37164*
[b]*Department of Engineering "Enzo Ferrari", University of Modena and Reggio Emilia, Via P. Vivarelli 10/1, 41125 Modena, Italy*
[c]*Pure and Applied Chemistry, University of Strathclyde, Glasgow G1 1BX, UK*
† Electronic supplementary information (ESI) available. See DOI: https://doi.org/10.1039/d3nr01512b

mechanical crashes in the primary stage, biodegradation in the secondary stage and chemical oxidation processes in the tertiary stage.[17]

Alternative removal strategies involve for example the silanisation of contaminated water to foster the coagulation of microplastics, using organosilane-based precursors, which have a high affinity to microplastics and high reactivity in water. Then, adding hybrid silica gels induces a sol–gel process, resulting in the fixation of microplastics into a three-dimensional networked hybrid silica gel, which is subsequently removed from the system.[18,19]

Apart from the separation of microplastic from aquatic systems, another intensely researched approach is to degrade plastic to either recover the monomers and recycle them,[20] or to mineralize the materials, which can be initiated through biological and non-biological processes. Using microorganisms to produce enzymatic reactions is a biological process that can lead to the degradation of microplastics. In this process, the enzyme attaches to the polymer structure of microplastics and degrades it into its monomer, which is later used by the microorganism for energy production.[21] On the other hand, photocatalysis is a non-biological process in which a photocatalytic material absorbs a light source's energy, producing an excited electron/hole pair that triggers a series of chemical reactions. Depending on the conditions of the process, different oxidant species are formed, which interact with the microplastics and degrade them until, ideally, their mineralization occurs.[22,23] The photocatalytic degradation of microplastics has gained relevance as it represents an alternative to transform microplastics into less toxic substances preventing persistent organic pollutants (POPs) and persistent, bioaccumulative and toxic (PBTs) into entering the tropic chain. Several works have investigated the photocatalytic degradation of polystyrene (PS) as a common share in microplastic waste, typically stemming from food packaging, building insulation, electrical and electronic appliances, among many others.[16] PS is very harmful to the environment.[24] Nabi *et al.* studied the photocatalytic degradation of PS spheres under UV light for 24 h, reporting a 99.9% degradation when the photocatalyst and PS microplastics were in film and a 40% degradation when the photocatalyst and PS microplastics were in dispersion.[25] Relatable results were obtained by Domínguez-Jaimes *et al.* who investigated the photocatalytic degradation of PS microplastics under UV light for 50 hours.[26] In this case, the photocatalyst was in a film and the PS microplastics were in dispersion, achieving 23.5% of microplastic elimination.[26] This indicates that the interaction between the photocatalyst and the microplastic particle is fundamental to increase the degradation efficacy.

Our innovative strategy to promote interaction between the photocatalyst and microplastics particles is using self-propelled micromotors to form motile microplastic rafts around them, which has been first investigated using self-propelling Au@TiO_2 Janus particles.[27] Wang *et al.* demonstrated that the phoretic interactions between the micromotors and microplastics made it possible for the micromotors to form clusters of microplastics and remove them, they reported a collection efficiency of 77% microplastics under UV light.[27] This rafting behaviour not only gave a physical understanding of the interactions between an active and passive particle,[28,29] but allowed the capture and removal of microplastics of different sizes and geometry.[27] The use of magnetic interactions for capture, joint with photocatalytic degradation was studied for different photocatalysts, combined with selected polymers.[30,31] Beladi-Mousavi *et al.* studied the potential of a $BiVO_4/Fe_3O_4$ photocatalyst to degrade different types of microplastics. A collection of 70% of polylactic acid (PLA) and polycaprolactone (PCL) microplastics was obtained under visible light exposure coupled with a magnetic field. Photocatalytic activity for the degradation of microplastics was also tested, achieving 3% degradation of PLA after 7 days of visible light irradiation.[31] Photocatalytic micromotors are envisioned to prove themselves a useful strategy for efficient removal of microplastics.[32] However, externally controlled magnetic capture is scalable only to a limited amount, for which we suggest phoretic interactions as intrinsic alternative.

To achieve that, we aim to combine the different principles that have been suggested to enhance the capture and degradation of PS microplastics in a single micromotor (Fig. 1). The first principle involves the enhanced ballistic motion generated by self-asymmetric micromotors,[33] the second involves micromotor-based collection of microplastics,[27] and the third is the photocatalytic degradation of microplastics.[22] To make this process scalable, we rely on inherently asymmetric microparticles with autonomous motion.[33] TiO_2-based Pac-Man-like microspheres were investigated for this purpose, as previous studies had already demonstrated optimal properties in photocatalytic activity and structural asymmetry, achieving a directed

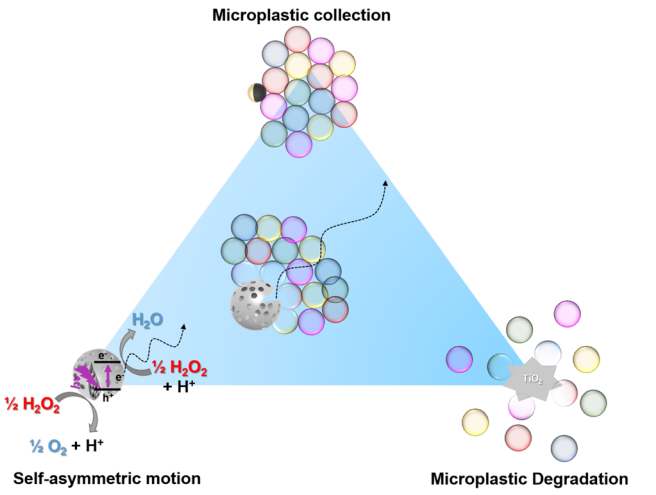

Fig. 1 Schematic illustration of our current photocatalytic micromotor-based system (at center) combining the principles of inherently self-asymmetric motion (bottom left), micromotor-based collection of microplastic (top), and photocatalytic degradation of microplastics (bottom right). The colorful translucent spheres represent polystyrene microparticles, and the transparent ones close to the photocatalyst (right and center) are degraded due to the photocatalytic action.

motion. Therefore, the proposed system successfully merges the collection and assembly of microplastics based on attractive phoretic interactions and their photocatalytic degradation.

2 Experimental section

2.1 Synthesis of Pac-Man TiO_2 particles

The synthesis of Pac-Man like particles is described in detail in previous publications.[33,34] Briefly, 4.57 w/v% of Pluronic P123 (M_n = 5800 g mol^{-1}, Sigma-Aldrich (Germany)) is taken in a 35 mL solvent mixture of acetic acid (100%, VWR chemicals (Germany)), hydrochloric acid (37 wt%, VWR chemicals (Germany)), and tetrahydrofuran (≥99.9%, Riedel-de Haën (Germany)) in volume ratio of 0.057 : 0.086 : 0.857. Following dissolution of the polymer in the solvent mixture, 3 mL of titanium(IV) butoxide (97%, Sigma-Aldrich (Germany)) and 200 μL of DI water are added dropwisely with continuous stirring. This solution is heated in a water bath at 40 °C for 24 h to obtain a transparent gel. 2 g of this gel is weighed in a 50 mL Teflon vessel and autoclaved at 70 °C for 24 h. The obtained white precipitate is washed with methanol, dried and calcined at 350 °C for 3 h in a N_2 atmosphere, followed by 3 h at 400 °C in air.

2.2 Material characterization

The Pac-Man morphology of these particles is observed using a scanning electron microscope (Zeiss Gemini SEM 300 instrument). The particles are also characterized by a powder X-ray diffractometer (Bruker 2D phaser powder X-ray diffractometer, Cu Kα radiation (30 kV, 10 mA) in the 2θ range of 5° to 100°), Fourier-transform infrared spectrometer (Thermo Scientific – Nicolet 8700 with attached Thermo Scientific Smart iTR in Attenuated Total Reflectance (ATR) mode) and diffuse reflectance spectrophotometer (Cary 5000 UV-Vis-NIR spectrophotometer), results are shown in the ESI, Fig. S1.†

2.3 Peroxide degradation and volume of O_2 evolved

The amount of O_2 evolved due to catalytic degradation of H_2O_2 by Pac-Man TiO_2 particles is measured by a self-designed drainage method inspired by Wang *et al.*[29] A schematic representation of the process is shown in ESI (Fig. S3†). For the experiment, a 1.5 mL quartz GC vial (from Nexus Company INC., Kyoto, Japan) is filled with 1 mL of a mixture of Pac-Man particles (1 g L^{-1}) in H_2O_2 (1%, or 2.5%, or 5%, or 10% (w/w)). The vial is then connected to a 1 mL glass gas syringe with a luer lock by a vial adapter and illuminated uniformly with UV LEDs (385 nm wavelength and intensity of around 250 mW cm^{-2} per LED (total 8 LEDs)). The amount of oxygen evolved is obtained by measuring the displacement of the piston in the glass syringe. At least 3 measurements are taken for each data point at a given H_2O_2 concentration. The volume of oxygen evolved is plotted against average time with standard deviation. The volume error of the glass syringe is calculated by weighting the obtained liquid amounts.

2.4 Motion experiments

The motion experiments with the Pac-Man particles are carried out directly without any further modification of the particles. Very dilute particle solution in DI water is prepared and motion videos at a frame rate of 40 fps are recorded using a camera (Zeiss camera (Axiocam 702 Mono)) attached to an inverted optical microscope (Axio observer from Carl Zeiss Microscopy GmbH). The motion studies are performed on a plasma cleaned glass slide at different peroxide concentrations, using UV light (19.08 W cm^{-2} intensity, 385 nm UV LED from Colibri 7 light source).[35] The speed from the motion videos are evaluated using Fiji (ImageJ), Matlab and analysed using Origin software. The speed of Pac-Man particles in different concentrations of H_2O_2 is represented in terms of a box plot, the left side of the plot depicts the box with interquartile range marking the 5th, 25th, 75th, and 95th percentile of the micromotor speed, the middle line is the median value of the speed. On the right half, the individual values of the speed are plotted. About 40–200 particles are tracked for each concentration.

2.5 Collective behavior of active Pac-Man TiO_2 colloids and passive polystyrene (PS) or SiO_2 microparticles

The collective assembly is based on the principle of phoretic interaction of catalytic self-propelling micromotor (active particles) with non-catalytic colloids (passive particles).[27] The active particles generate a local gradient (chemical/electrical) due to the asymmetric degradation of the fuel inducing local and confined interaction.[36] These interactions are non-selective and independent of the size and type of passive particles (Fig. S4†).[27] Thus this interaction behavior can be easily adapted to other types of microplastics.[27]

In this manuscript, we used 2 μm, 5 μm PS (10 wt%), and 2 μm SiO_2, commercially obtained from Sigma-Aldrich (Germany). SiO_2 microparticles are typical passive particles used in interaction studies as it facilitates 2D assembly close to the glass substrate.[37,38] For active-passive interaction study, 10 wt% of 5 μm PS, 0.05 wt% of 2 μm PS and 0.05 wt% of 2 μm SiO_2 are prepared. Next, on a cleaned glass slide (plasma cleaned glass slides, precleaned with acetone and isopropanol), 1 μL aqueous solution of Pac-Man TiO_2 microparticles is added followed by 10 μL passive microparticles and 10 μL of H_2O_2 of different concentrations. After the particles are settled, the solution is irradiated with UV light (19.08 W cm^{-2} intensity, 385 nm UV LED from Colibri 7 light source),[35] and images are captured at definite time intervals (0, 30, 60, 120, 300 and 600 s) using an inverted optical microscope. The number of passive particles in the cluster is calculated manually by Fiji using the "cell counter" plugin.

2.6 Dye degradation

The photocatalytic activity of Pac-Man particles is evaluated by the degradation of rhodamine B (RhB), a model organic dye for photocatalytic reactions.[39] Prior to the photodegradation experiment, an aqueous solution of RhB (0.01 mM, 15 mL) is

taken in a glass beaker together with Pac-Man microparticles (1 mg mL^{-1}), which is then magnetically stirred in dark for 30 minutes to reach adsorption–desorption equilibrium of the dye on the catalyst surface. After the dark reaction, the solution is placed under a UV lamp (hand UV lamp from Herolab GmbH, Germany, lamp intensity 950 μW cm^{-2} and wavelength 365 nm) under magnetic stirring. The residual concentration (C) is noted after every 5 minutes for a 30 minutes time interval by measuring the absorbance intensity at its maximum absorbance wavelength of 553 nm. C_0 is the initial concentration and is taken at t = 0 min (before irradiating with UV light). Measurements are taken in an absorbance range of 450 nm to 650 nm using a UV-visible spectrometer (Cary 60, Agilent Technologies) and in 1 cm path length quartz cuvette. A control sample is prepared in absence of the catalyst and measured under the same experimental conditions. The dye degradation efficiency (%) is determined as:

$$\text{dye degradation efficiency}\,\% = \frac{C_0 - C}{C_0} \times 100\% \qquad (1)$$

2.7 Photocatalytic degradation of microplastics

Polystyrene (PS) microparticles (2 μm and 5 μm, 10 wt%) are used for the microplastic degradation studies. Briefly, 0.4 wt% PS is prepared by washing and dispersing the stock particles in 100 μL water. Similarly, a dispersion of 100 mg mL^{-1} of Pac-Man TiO_2 is prepared in 100 μL of water. Both these aqueous suspensions of PS and TiO_2 are mixed together in a 1 : 1 ratio and sonicated. 10 μL of this mixture is then drop-casted on a small Petri dish, filled with 5 mL H_2O_2 in different concentrations (1%, or 2.5%, or 5%, or 10% (w/w)) and placed in UV light (hand UV lamp from Herolab GmbH, Germany, lamp intensity 950 μW cm^{-2} and wavelength 365 nm) for 70 h. The distance between the sample and the UV lamp is fixed at 5 cm (Fig. S8†). To promote the continued motion and photocatalytic degradation and avoid complete evaporation of H_2O_2, 3 mL of H_2O_2 (maintaining the concentration) are added every 24 hours. After UV irradiation, the particles are rinsed with ethanol and are imaged using SEM.

2.7.1 Evaluation based on size change of polystyrene microparticles. The size change after the degradation (D) is measured by comparing the diameter (Fig. S9†) of PS particles from the SEM images using Fiji software. At least 35 PS particles are imaged for each case. Control samples are also prepared for both PS sizes without TiO_2 particles at 10% w/w H_2O_2, keeping the other degradation conditions same. The degradation efficiency is calculated by:

$$\text{PS degradation efficiency}\,\% = \frac{D_0 - D}{D_0} \times 100\% \qquad (2)$$

The as-obtained commercial PS particles are imaged and are taken as the initial diameter (D_0, blank). Statistical treatment on the average diameter change of microplastic particles after degradation is performed using a one-way ANOVA test in excel and is shown in ESI.†

2.7.2 Evaluation based on carbonyl absorption band. PS undergoing a typical oxidative degradation pathway forms polar functional groups such as ketones and ester carbonyls which can be detected by FTIR.[40,41] The higher intensity in carbonyl bands does not always imply a higher extent of degradation, so it is compared with a reference band such as the C–H band which is unaffected due to degradation.[42] The extent of degradation is further quantified by calculating the carbonyl index defined as the ratio of carbonyl band (around 1720 cm^{-1}) to aromatic C–H stretching (2850 cm^{-1}) (CI = A_{1720}/A_{2850}). At least 3 measurements were made for each degradation case and the residual absorbance is plotted with respect to blank with a standard deviation. The residual concentration (C or CI) is plotted over the initial concentration (C_0, CI of blank PS), the results are presented in ESI, Fig. S14.†

3 Results and discussion

As previously described, the synthesized TiO_2 microparticles form with a crack due to the release of accumulated stress from the solvent vapors (Fig. 2A, inset SEM image).[34] In combination with the photocatalytic properties, this geometry allows these Pac-Man TiO_2 particles to generate an asymmetric fluid flow around them and propel autonomously. In comparison to traditional Janus particle micromotors, this fabrication yields active particles without any asymmetrisation step or the requirement of expensive noble metals.

H_2O_2 serves as fuel for (photo)catalytic motion and degradation, TiO_2 photodissociates H_2O_2 to oxygen which can be measured to understand the photocatalytic activity of Pac-Man TiO_2 particles at different peroxide concentrations. To evaluate the correlation of catalytic H_2O_2 degradation activity with the swimming speed, we designed a gas evolution setup (see Fig. S3†). The sample is irradiated homogeneously using a cylindrical arrangement of 8 LEDs of intensity 0.25 W cm^{-2} per LED and the generated gas is collected as oxygen evolution test. For practical reasons we measure the activity in terms of the time taken to evolve a certain volume of oxygen in different concentrations of H_2O_2. As expected the turnover number increases with an increase in H_2O_2 concentration, resulting in shorter times required to evolve the same volume of oxygen (Fig. 2A). The active motion of Pac-Man particles is observed in the presence of H_2O_2 irradiated with UV light through the objective of the microscope. Even at low H_2O_2 concentration of 1% they propel autonomously and the speed progressively increases with increasing H_2O_2 concentration (Fig. 2B, speed trajectories (top)). It becomes apparent from the individual values on the right sides of the box plot, that the spread of values also increases with the peroxide concentration (Fig. 2B, Video S1†). The dependence of the Pac-Man particles on fuel concentration is also observed from the mean-square displacement graph (Fig. S2†). As the fuel concentration increases, the particles exhibit a robust ballistic regime and directed motion, whereas, in the absence of H_2O_2, the particles show just Brownian movement.

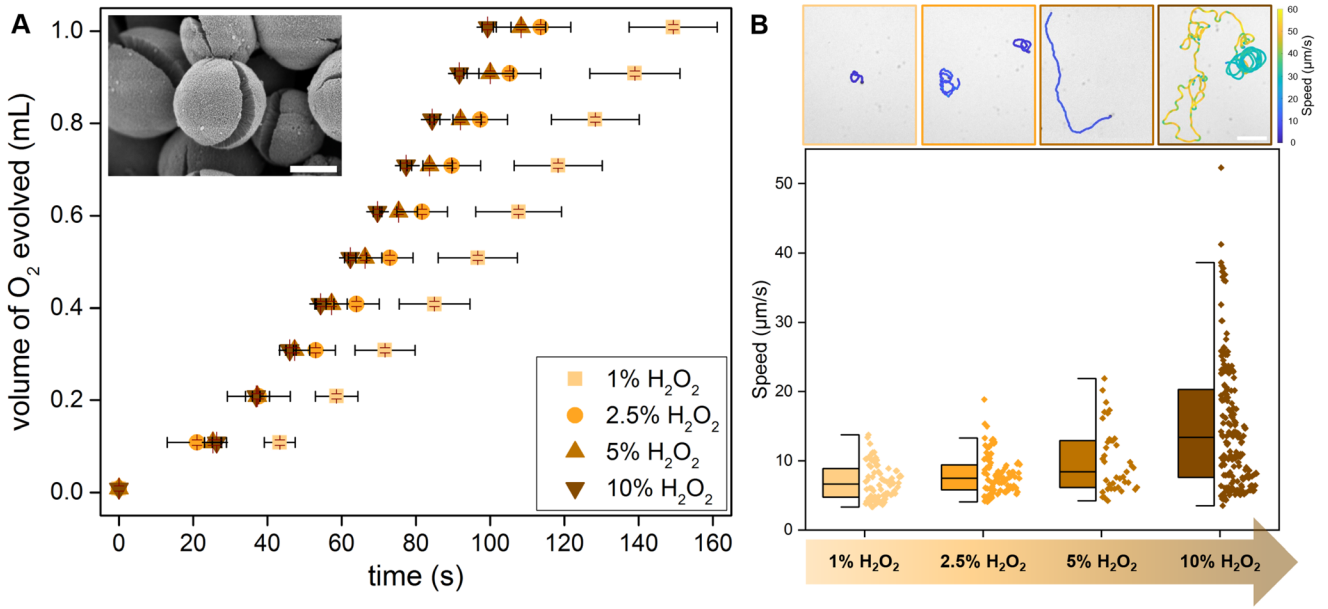

Fig. 2 Correlation between (A) photocatalytic activity of Pac-Man particles measured in terms of time taken to evolve distinct volumes of oxygen and (B) optical images showing trajectories of motion for single particle for 575 frames at different H_2O_2 concentration. The trajectories are color coded according to instantaneous speed and box plots of speed values for at least 40 motile particles for each H_2O_2 concentration. Scale bar in the trajectories is 20 μm. Inset in figure (A) shows a SEM image of Pac-Man TiO_2 microparticles, scale bar is 1 μm. UV light is used of wavelength 385 nm and intensity 0.25 W cm^{-2} of each LED (total 8 LEDs) and 19.08 W cm^{-2} for oxygen evolution study and microscope experiments respectively.

3.1 Active–passive interactions

However, we conjecture these particles produce an effectively pusher-like flow field,[43] based on the individual particle behaviours. This made us optimistic that the Pac-Man particles would emulate the rafting behavior shown by Au@TiO_2 Janus micromotors. Replacing them with our Pac-Man microparticles, leads to a scalable base for efficient interaction and capture of microplastics.

Actively swimming Pac-Man particles interacted with passive suspended matter, forming increasingly large clusters over time. Similar to their Janus analogues, the raft size is also directly dependent on activity and can be increased with the concentrations of H_2O_2 (Fig. 3A). Snapshots of the assembly process are simultaneously shown for some H_2O_2 concentrations and time intervals (Fig. 3B, Video S2†). Despite the slower average speeds, the formed dynamic clusters reach similar magnitudes compared to the clusters assembled by Janus micromotors in Wang *et al.*[29] While in the initial seconds the clusters experience rapid growth, the number seems to plateau into non-equilibrium stable states.[29] The clustering and assembly behavior is robust and observed for a variety of materials,[29] here we only test passive polystyrene particles of different sizes (2 and 5 μm) (Fig. S5†). For the number

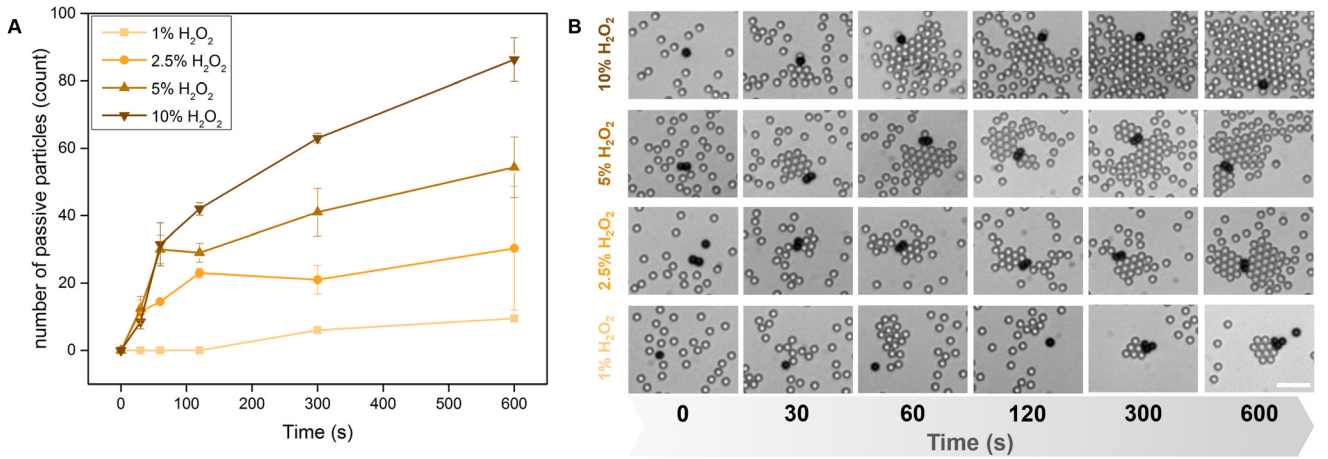

Fig. 3 (A) Quantification of rafting behavior with SiO_2 colloids and (B) optical microscopy snapshots after different time intervals at different H_2O_2 concentrations. A UV light of intensity 19.08 W cm^{-2} and wavelength 385 nm is used.

determination in Fig. 3 we used SiO_2 particles to facilitate counting of raft participants because the assembly takes place in a single plane (2D), while the lower density of PS spheres favors 3D assembly.

3.2 Degradation of organic dye and microplastics

In order to test the viability of using a single material for both, capture and degradation of microplastics, we will evaluate the capability of the Pac-Man particles to decompose the polymer, which has been observed for a range of plastics in combination with photocatalysts.[23,44] Looking at articles that pioneered the degradation of microplastics using advanced oxidative processes (AOPs), we clearly noticed a lack of suitable analytics to measure the activity. Therefore, we evaluate the photocatalytic degradation of an organic dye (Rhodamine B (RhB)), which is, as opposed to the degradation of microplastics, easily traceable by measuring the light absorption. RhB has a characteristic absorption peak at 553 nm and thus the degradation is observed within the absorbance range of 450 nm to 650 nm. The photodegradation of the dye is performed in presence of Pac-Man TiO_2 particles (1 g L^{-1}) and UV light (950 μW cm^{-2} intensity and 365 nm wavelength). Before the degradation study, the catalyst is stirred with the dye solution for 30 minutes in order to reach an adsorption equilibrium within the pores of the catalyst, also noted by a slight decrease in absorbance of the dye (Fig. 4A).

When irradiated with light, the concentration of the dye (C/C_0) decreases with time and a degradation of around 53% is attained in 30 minutes (Fig. 4B). The degradation experiments were conducted in absence of H_2O_2 as photo-oxidation of RhB can take place in presence of UV light and H_2O_2.[45] To resume, the photodecomposition of RhB is reflected by a decrease in the residual concentration of the dye in presence of Pac-Man particles, proving the photocatalytic activity (beyond active propulsion) (Fig. S6 & S7†). These results demonstrate that the Pac-Man particles display a superior photocatalytic activity compared to TiO_2 Degussa P-25. It has been reported that 30 nm Degussa P-25 photocatalyst degrades around 40% of RhB in 30 min.[46] Even though the difference in degradation may not seem significant, it is worth noting that a bigger particle size of the photocatalyst can affect negatively its photocatalytic activity. This phenomenon was described by Wilhelm and Stephan,[47] who studied the photocatalytic degradation of RhB using SiO_2@TiO_2 spheres of different sizes and titania nanosol. They observed that increasing the particle size decreased the RhB degradation as the specific surface area was smaller. Therefore, for a particle with particle size in the range of micrometers, it is needed a far superior photocatalytic activity to eliminate the same amount of pollutant than a 30 nm particle.

To investigate the degradation of microplastics we selected spherical, homogeneous polystyrene particles of sizes 2 μm and 5 μm to facilitate quantitative analysis of SEM images. In order to observe significant degradation of microplastics in contact with the catalytic Pac-Man particles, we selected UV irradiation and H_2O_2, *i.e.* the ideal swimming environment for Pac-Men. The extent of degradation is evaluated from the morphological changes in the polystyrene (PS) particles, an

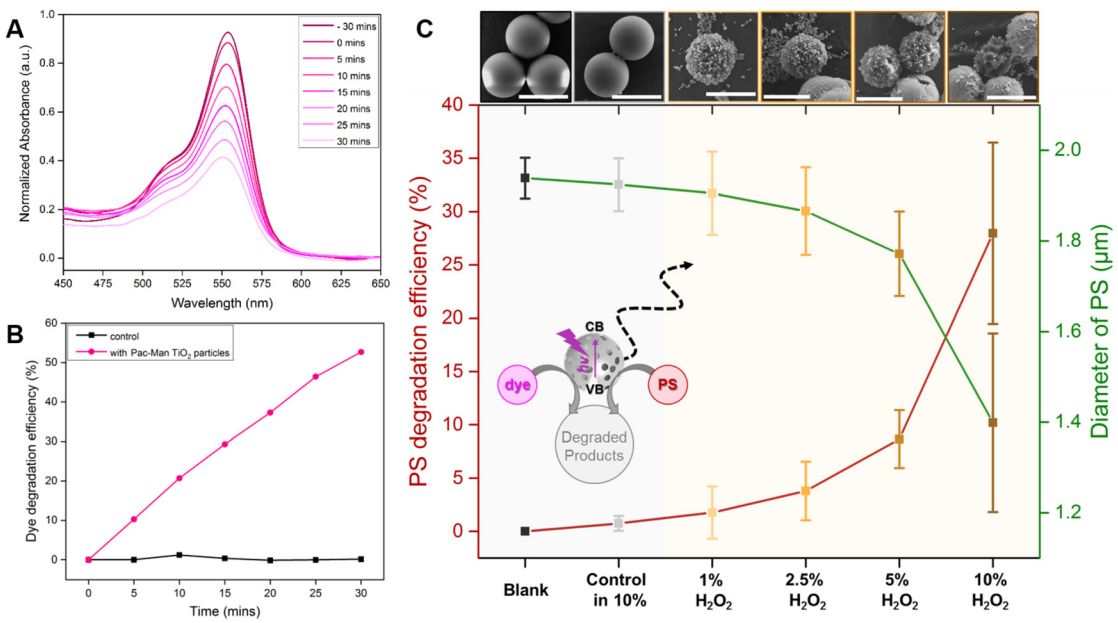

Fig. 4 (A) UV-vis spectra showing the degradation of RhB in presence of Pac-Man TiO_2 microparticles. (B) Dye degradation efficiency of the photocatalyst as a function of irradiation time is compared with the control. Concentration of TiO_2 and RhB is 1 mg mL^{-1} and 0.01 mM respectively. (C) Average degradation efficiency and diameter change (imaged using SEM) of 2 μm PS particles after treating with Pac-Man in different H_2O_2 concentrations. Degradation of a control sample is also compared at the highest H_2O_2 concentration of 10% (w/w). A constant degradation time of 70 h is maintained for each case. Concentration of TiO_2 and microplastics is 50 mg mL^{-1} and 0.2 wt%. In both RhB and PS degradation studies, a UV hand lamp of intensity 950 μW cm^{-2} intensity with a wavelength of 365 nm is used.

approach that has been used by other authors.[25] After 70 h of degradation experiment, in different peroxide concentrations, the morphology of the PS is studied by SEM. The average diameter of the polystyrene and the respective efficiency of degradation are calculated with regard to the blank sample. Foreseeably, with a higher H_2O_2 concentration, a greater extent of degradation occurs. The extent of PS degradation is prominently visible from an example SEM image of each case shown in Fig. 4C (top). In presence of the catalyst and H_2O_2, the PS microparticles degrade and become more irregular and rough with pores, holes, and punctures formed due to the degradation process. The degradation is quantified in terms of the averaged diameter change of the PS. As the concentration of H_2O_2 is increased, a higher decrease in PS diameter is observed, a decrease of around 0.54 μm is attained at the highest H_2O_2 concentration (10%) with a degradation efficiency of around 28% (Fig. 4C). To validate that the degradation is enforced by the catalytic activity of Pac-Man TiO_2 particles at higher H_2O_2 concentration, a control sample in absence of catalyst is also studied at the highest H_2O_2 concentration (10%) with same experimental conditions, showing merely a degradation of around 0.7% without any significant change in the morphology of the PS (Fig. 4C). Degradation studies are also carried out with 5 μm PS particles, a similar effect is observed *i.e.* higher degradation efficiency at higher concentration of H_2O_2 but at much lower extent compared to 2 μm PS particles (~7% degradation at 10% H_2O_2) (Fig. S11 & 12†). The statistical significance of the microplastic degradation experiment by the size-change study is provided separately in ESI (Fig. S13†). CI of both PS particles after photodegradation is also studied (Fig. S14†).

The different time scales of all degradable substrates, from H_2O_2 in the order of ms or smaller, leading to fluid flows, crossing RhB degrading in the order of minutes to the polymeric substrates, that require extended reaction times of several days, show the versatility of the TiO_2 catalyst. This versatility enables the use of a single compound particle for propulsion, raft generation and plastic degradation.

4 Conclusions

We could show, that an easy to fabricate, single compound micromotor can form rafts that enable microplastics collection and beyond that, the same material accelerates the degradation of the polymer material to a viable extend. Results indicate that Pac-Man particles interact with PS particles forming dynamic clusters even after extended periods of UV light activation when H_2O_2 is present in the system. Additionally, Pac-Man particles could degrade up to 28% of PS particles after 70 h of UV light exposure.

In order to characterise the partial degradation we quantitatively evaluate size changes, following a multi-directional image-based particle diameter evaluation (>30 particles for each case), which represents a significant methodological improvement to status-quo. The detection and quantification of microplastics in general, as well as the degradation is still a challenging aspect and in the near future significant progress through coordinated research initiatives is expected.

The time discrepancy between swimming (in the order of seconds), dye degradation and PS degradation (~250 ks) is unavoidable using a single catalyst material due to different stabilities and degradation kinetics, we envision a future micromotor that collects the microplastics into a small chamber with intense irradiation in order to upconcentrate and subsequently degrade them. We conjecture that maintaining the one-pot synthesis strategy, but tuning the catalytic activity (*e.g.* by doping), which will improve both, the swimming activity (and thereby enhancing the collection activity) as well as the speed of polymer degradation, but is out with the scope of this paper. Microplastic pollution remains one of the emerging concerns for the environment with absence of strategic solutions. While we are clearly not yet presenting a viable solution to the global microplastics problem, we showed that TiO_2 Pac-Men as scalable, noble metal free type of active particle have the potential to become a game-changing strategy unifying microplastics collection and degradation. Future studies have to focus on the fate of the degraded products on the marine organisms to better evaluate the applicability of the system and avoid the creation of additional threads.

Author contributions

Conceptualization, JS; measurements and analysis, PC and MCAT; measurement supervision, JS; writing – original draft preparation, PC, MCAT, JS; writing – review and editing, JS, EICG, CS; project administration, JS; funding acquisition, JS, MCAT, EICG, CS. All authors have read and agreed to the final version of the manuscript.

Conflicts of interest

The authors have no conflicts to declare.

Acknowledgements

We are grateful for a Freigeist grant (No. 91619) from the Volkswagen foundation and a Fulbright Cottrell Award and the Green Talents program, which partially supported this study. PC would like to acknowledge Free state of Saxony represented by state parliament for Saxon fellowship and also Graduate Academy, TU Dresden. MCAT acknowledges the BMBF for the Green Talents Award. All authors acknowledge Linlin Wang, who pioneered the microplastic rafting, for initial discussions and our BSc students Rowan Fairweather Graham and Jean Andrew for proof reading.

References

1 PlasticsEurope, *Plastics—the facts 2010. An analysis of European plastics production, demand and recovery for 2009*, 2010.
2 PlasticsEurope, *Plastics—the facts 2022*, 2022.
3 J. Wang, Z. Tan, J. Peng, Q. Qiu and M. Li, *Mar. Environ. Res.*, 2016, **113**, 7–17.
4 M. Bergmann, L. Gutow and M. Klages, *Marine anthropogenic litter*, Springer Nature, 2015.
5 K. Zhang, A. H. Hamidian, A. Tubić, Y. Zhang, J. K. Fang, C. Wu and P. K. Lam, *Environ. Pollut.*, 2021, **274**, 116554.
6 L. Lebreton and A. Andrady, *Palgrave Commun.*, 2019, **5**, 1–11.
7 M. MacLeod, H. P. H. Arp, M. B. Tekman and A. Jahnke, *Science*, 2021, **373**, 61–65.
8 N. B. Hartmann, T. Huffer, R. C. Thompson, M. Hassellöv, A. Verschoor, A. E. Daugaard, S. Rist, T. Karlsson, N. Brennholt and M. Cole, *et al.*, *Are we speaking the same language? Recommendations for a definition and categorization framework for plastic debris*, 2019.
9 A. L. Andrady, *Mar. Pollut. Bull.*, 2011, **62**, 1596–1605.
10 M. C. Rillig and A. Lehmann, *Science*, 2020, **368**, 1430–1431.
11 G. Chen, Q. Feng and J. Wang, *Sci. Total Environ.*, 2020, **703**, 135504.
12 M. S. Bank and S. V. Hansson, *Microplastic in the Environment: Pattern and Process*, 2022, pp. 1–16.
13 C. M. Rochman and T. Hoellein, *Science*, 2020, **368**, 1184–1185.
14 Z. Long, Z. Pan, W. Wang, J. Ren, X. Yu, L. Lin, H. Lin, H. Chen and X. Jin, *Water Res.*, 2019, **155**, 255–265.
15 A. M. Elgarahy, A. Akhdhar and K. Z. Elwakeel, *J. Environ. Chem. Eng.*, 2021, **9**, 106224.
16 A. Tursi, M. Baratta, T. Easton, E. Chatzisymeon, F. Chidichimo, M. De Biase and G. De Filpo, *RSC Adv.*, 2022, **12**, 28318–28340.
17 X. Wu, X. Zhao, R. Chen, P. Liu, W. Liang, J. Wang, M. Teng, X. Wang and S. Ga, *Water Res.*, 2022, 118825.
18 K. Schuhen, M. T. Sturm and A. F. Herbort, *Plast. Environ.*, 2019, 1–16.
19 M. T. Sturm, H. Horn and K. Schuhen, *Water*, 2021, **13**, 675.
20 C. Jönsson, R. Wei, A. Biundo, J. Landberg, L. Schwarz Bour, F. Pezzotti, A. Toca, L. M. Jacques, U. T. Bornscheuer and P.-O. Syrén, *ChemSusChem*, 2021, **14**, 4028–4040.
21 A. R. Othman, H. A. Hasan, M. H. Muhamad, N. I. Ismail and S. R. S. Abdullah, *Environ. Chem. Lett.*, 2021, **19**, 3057–3073.
22 M. C. Ariza-Tarazona, J. F. Villarreal-Chiu, V. Barbieri, C. Siligardi and E. I. Cedillo-González, *Ceram. Int.*, 2019, **45**, 9618–9624.
23 M. C. Ariza-Tarazona, J. F. Villarreal-Chiu, J. M. Hernández-López, J. R. De la Rosa, V. Barbieri, C. Siligardi and E. I. Cedillo-González, *J. Hazard. Mater.*, 2020, **395**, 122632.
24 J. Hwang, D. Choi, S. Han, S. Y. Jung, J. Choi and J. Hong, *Sci. Rep.*, 2020, **10**, 1–12.
25 I. Nabi, K. Li, H. Cheng, T. Wang, Y. Liu, S. Ajmal, Y. Yang, Y. Feng, L. Zhang, *et al.*, *iScience*, 2020, **23**, 101326.
26 L. P. Domínguez-Jaimes, E. I. Cedillo-González, E. Luévano-Hipólito, J. D. Acuña-Bedoya and J. M. Hernández-López, *J. Hazard. Mater.*, 2021, **413**, 125452.
27 L. Wang, A. Kaeppler, D. Fischer and J. Simmchen, *ACS Appl. Mater. Interfaces*, 2019, **11**, 32937–32944.
28 I. P. Madden, L. Wang, J. Simmchen and E. Luijten, *Small*, 2022, **18**, 2107023.
29 L. Wang and J. Simmchen, *Soft Matter*, 2023, **19**, 540–549.
30 W. Li, C. Wu, Z. Xiong, C. Liang, Z. Li, B. Liu, Q. Cao, J. Wang, J. Tang and D. Li, *Sci. Adv.*, 2022, **8**, eade1731.
31 S. M. Beladi-Mousavi, S. Hermanova, Y. Ying, J. Plutnar and M. Pumera, *ACS Appl. Mater. Interfaces*, 2021, **13**, 25102–25110.
32 M. Urso and M. Pumera, *Adv. Funct. Mater.*, 2022, **32**, 2112120.
33 P. Chattopadhyay, S. Heckel, F. Irigon Pereira and J. Simmchen, *Adv. Intell. Syst.*, 2022, 2200091.
34 K. Lan, R. Wang, W. Zhang, Z. Zhao, A. Elzatahry, X. Zhang, Y. Liu, D. Al-Dhayan, Y. Xia and D. Zhao, *Chem*, 2018, **4**, 2436–2450.
35 S. Heckel, M. Wittmann and J. Simmchen, *Zenodo*, 2021, 1–2.
36 L. Wang and J. Simmchen, *Condens. Matter*, 2019, **4**, 78.
37 D. P. Singh, U. Choudhury, P. Fischer and A. G. Mark, *Adv. Mater.*, 2017, **29**, 1701328.
38 Y. Gao, F. Mou, Y. Feng, S. Che, W. Li, L. Xu and J. Guan, *ACS Appl. Mater. Interfaces*, 2017, **9**, 22704–22712.
39 P. Chattopadhyay, T. Gemming, A. Eychmüller and J. Simmchen, *J. Phys. Chem. C*, 2021, **125**, 24887–24893.
40 A. Chamas, H. Moon, J. Zheng, Y. Qiu, T. Tabassum, J. H. Jang, M. Abu-Omar, S. L. Scott and S. Suh, *ACS Sustainable Chem. Eng.*, 2020, **8**, 3494–3511.
41 T. J. Kemp and R. A. McIntyre, *Polym. Degrad. Stab.*, 2006, **91**, 3010–3019.
42 A. D. Vital-Grappin, M. C. Ariza-Tarazona, V. M. Luna-Hernández, J. F. Villarreal-Chiu, J. M. Hernández-López, C. Siligardi and E. I. Cedillo-González, *Polymers*, 2021, **13**, 999.
43 S. Heckel, C. Bilsing, M. Wittmann, T. Gemming, L. Büttner, J. Czarske and J. Simmchen, *Adv. Sci.*, 2022, **9**, 2105009.
44 H. Du, Y. Xie and J. Wang, *J. Hazard. Mater.*, 2021, **418**, 126377.
45 F. H. AlHamedi, M. Rauf and S. S. Ashraf, *Desalination*, 2009, **239**, 159–166.
46 T. S. Natarajan, M. Thomas, K. Natarajan, H. C. Bajaj and R. J. Tayade, *Chem. Eng. J.*, 2011, **169**, 126–134.
47 P. Wilhelm and D. Stephan, *J. Photochem. Photobiol., A*, 2007, **185**, 19–25.